

EQUILIBRIUM-STATE DENSITY PROFILES OF CENTRIFUGED CAKES OF FLOCCULATED SUSPENSIONS

WEI-HENG SHIH,* WAN Y. SHIH,** SEONG-IL KIM,# and ILHAN A. AKSAY**

*Department of Materials Engineering, Drexel University, Philadelphia, PA 19104;

**Department of Chemical Engineering, and Princeton Materials Institute, Princeton University, Princeton, NJ 08544; #Ferro Corporation, Santa Barbara, CA 93117.

INTRODUCTION

Many advanced ceramics are formed by colloidal consolidation using techniques such as sedimentation, centrifugation, or pressure filtration. In all these, the minimization of density variations of various colloidally-consolidated cakes has not been examined systematically until recently. Schilling et al.¹ used γ -ray densitometry to study the density variations in a sedimented cake and showed that the sediment of a flocculated alumina suspension exhibited significant density variations within the cake whereas the sediment of a dispersed alumina suspension showed a constant density profile. Auzeais et al.² used a medical X-ray computer tomography (CT) to study the settling of dispersed and flocculated silica suspensions and obtained similar results: The sedimented cake of a dispersed silica suspension was fairly uniform whereas those of flocculated silica suspensions exhibited significant density variations.² However, Shih et al.³ examined pressure-filtered cakes of flocculated alumina suspensions with γ -ray densitometry and showed that the density profiles of pressure-filtered cakes of flocculated alumina suspensions were uniform,³ in contrast to their sedimentation counterparts which showed significant density variations.¹ These studies illustrate that how the local density varies within a consolidated cake depends not only on the suspension conditions but also on how the suspensions are consolidated, e.g., the consolidation pressure.

The goal of this paper is to examine the equilibrium-state density profiles of centrifuged cakes of flocculated suspensions both theoretically and experimentally. The emphasis is to take into account the effect of the consolidation pressure by relating the equilibrium-state density profiles to the pressure-cake-density relationship. By equilibrium state we mean the stage in which the cake height no longer changes with time. Theoretically, the equilibrium-state density profiles of centrifuged cakes were obtained by implementing the experimentally obtained pressure-density relationships into the general differential equations and solving the differential equations with appropriate boundary conditions. Experimentally, the density profiles were examined by γ -ray densitometry.¹

EXPERIMENTAL

The ceramic powders used in this study were α -alumina (AKP-30) powders supplied by Sumitomo Chemical Company in Osaka, Japan and boehmite powders by Vista Chemical Co. in Houston, Texas. The median diameter of AKP-30 is 0.4 μm . The boehmite powders are agglomerated platelike crystallites. The dry agglomerates are irregular in shape with an average size of about 65 μm . The agglomerates can be dispersed in acidic solutions and broken up into single crystallites (50-100 \AA in diameter and 10-20 \AA in thickness) or small agglomerates. Powder suspensions were prepared by electrostatic stabilization. Both alumina and boehmite suspensions were prepared under the flocculation conditions, i.e., boehmite at pH = 5.5 and 7.0 and alumina at pH = 7.0, respectively.

The centrifugation experiments were done with an IEC Model CL Centrifuge by Damon/IEC Division at Needham Heights, Massachusetts. The distance from the center of rotation to the bottom of the tube was $R = 13.92$ cm. The centrifugation frequency ranged from

$\omega = 48$ to $\omega = 241$ rad/sec, resulting in a corresponding gravitational force ranging from 32.8 g to 824.3 g at the bottom of the tube where g denotes the acceleration of gravity.

The density profiles of centrifuged cakes were obtained by γ -ray transmission measurements performed with a 3.2 mm diameter beam of collimated photons of 661 keV from Cesium 137 immediately after the samples were removed from the centrifugation unit. The average density at each elevation was calculated using the Beer-Lambert law.¹

PRESSURE-DENSITY RELATIONSHIP

The mean compressive pressure $P_{s,m}$ of an equilibrium-state centrifuged cake from a flocculated suspension has been shown^{3,5-6} to be a power-law function of the average density ϕ_{ave} as:

$$P_{s,m} = \beta \phi_{ave}^n, \quad (1)$$

where $P_{s,m} = (R - h/2) \omega^2 \Delta\rho h_0 \phi_0 / 2$ with R being the distance from the bottom of the cake to the center of rotation, h the cake height, ω the angular centrifugation frequency, $\Delta\rho$ the mass density difference between the solid and the fluid, and h_0 and ϕ_0 the initial suspension height and the initial suspension density, respectively. The numerical values of β , n , h_0 and ϕ_0 for the present experimental systems are listed in Table I. As can be seen in Table I, the coefficient β and the exponent n depend on a number of factors such as the suspension pH, the particle size, the materials and the initial suspension density.^{3,4} The initial-suspension-density dependence is shown between the two sets of boehmite cakes at pH = 7.0. The power-law dependence of $P_{s,m}$ on ϕ_{ave} is a manifestation of the fractal nature of the flocs that pack to form the cake⁵ and is indicative of the lack of network restructuring that occurs in pressure filtration.^{3,4,6} Generally, the value of n decreases as the degree of flocculation increases. Among the three suspension conditions examined, the boehmite suspensions at pH = 5.5 are the most strongly flocculated as evidenced by their linear viscoelasticity, low gelation densities and low sediment densities.⁵ The boehmite suspensions at pH = 7.0 are the second most flocculated and the alumina suspensions at pH = 7.0 are the least flocculated among the three. As we show below, the density profiles of the cakes are closely related to the n value.

	β (MPa)	n	ϕ_0 (vol%)	h_0 (cm)
Alumina, pH=7.0	1.73×10^2	8.9	14.82	7.88
Boehmite, pH=7.0	1.33×10^3	3.6	0.88	8.1
Boehmite, pH=7.0	1.364×10^3	4.0	2.25	7.6
Boehmite, pH=5.5	0.46	1.44	0.94	8.22

Table I: Values of β , n , ϕ_0 , h_0 , for centrifuged cakes of alumina at pH = 7.0 and boehmite at pH = 7.0 and 5.5 where β is the coefficient and n the exponent of Eq. (1), and ϕ_0 , and h_0 are the initial suspension height and the initial suspension density, respectively.

THEORY

In the equilibrium state of a centrifugation process, the cake height does not change with time, which indicates that there is neither material flow nor fluid flow in the centrifugation tube. Under such conditions, the general differential equation for centrifugation in cylindrical coordinates is reduced to⁷

$$\frac{dP_s}{dr} + (1 - k_0) \frac{P_s}{r} = \Delta\rho\phi\omega^2 r, \quad (2)$$

where r denotes the distance from the center of rotation, P_s the compressive pressure on the solid network in the cake, ϕ the volume fraction of the solid, k_0 the coefficient of lateral pressure defined as the ratio of the horizontal pressure to the vertical pressure. A typical value of k_0 for granular materials is about 0.5. Using Eq. (1) to approximate the relationship between P_s and ϕ , we obtain

$$\phi(z) = [a_1(R-z)^2 + a_2(R-z)^b]^{1/(n-1)}. \quad (3)$$

where $a_1 = [(n-1)\omega^2(\Delta\rho/\beta)]/[2n+(n-1)(1-k_0)]$, $b = (n-1)(1-k_0)/n$, both of which can be deduced from the experimental input, a_2 a constant to be determined by the boundary conditions and z is the distance measured from the bottom of the cake.

Meanwhile, in a centrifugation process, a supernatant will always be present. Since the solid content in the supernatant is negligible, the density of the top portion of a centrifuged cake must drop significantly to merge with that of the supernatant. If we let z_m be the distance from the bottom of the cake at which ϕ vanishes, the density profile of a centrifuged cake must obey the following two boundary conditions:

$$\phi(z_m) = 0, \quad (4)$$

and

$$\int_0^{z_m} \phi(z) dz = \phi_0 h_0. \quad (5)$$

With the known values of a_1 and b and the boundary conditions Eqs. (4) and (5), one can solve for a_2 and z_m and thus, the entire density profile. Moreover, if we let $\phi_{\max} \equiv \phi(z=0)$ be the density at the bottom of the cake, the relative density $\phi(z)/\phi_{\max}$ can be expressed in terms of z/R and z_m/R as

$$\left(\frac{\phi(z)}{\phi_{\max}}\right)^{n-1} = \frac{\left(1-\frac{z}{R}\right)^2 - \left(1-\frac{z_m}{R}\right)^{2+b} \left(1-\frac{z}{R}\right)^{-b}}{1 - \left(1-\frac{z_m}{R}\right)^{2+b}}. \quad (6)$$

Both z and z_m are much smaller than R . Expanding $[\phi(z)/\phi_{\max}]^{n-1}$ to first order in z/R and z_m/R , we arrive at a rather simple expression between $\phi(z)/\phi_{\max}$ and z/z_m , i.e.,

$$\phi(z)/\phi_{\max} \equiv (1-z/z_m)^{1/(n-1)}. \quad (7)$$

In fact, Eq. (7) is a very good approximation for the density profiles of centrifuged cakes. The higher-order terms of $\phi(z)/\phi_{\max}$ in z/R and z/z_m turn out to be insignificant even near $z = z_m$.⁸ One can clearly see from Eq. (7) that the exponent n in the pressure-density relationship is the most crucial parameter in determining how the relative density $\phi(z)/\phi_{\max}$ changes with the relative distance z/z_m .

RESULTS

To compare both the calculated density profiles with the experimental ones, we first plot $\phi(z)/\phi_{\max}$ versus z/z_m in Fig. 1 in which there are three sets of curves. Set (a) is for alumina cakes at pH = 7.0. The solid line, the open triangles and the open squares represent the calcu-

lated curves for $\omega = 241$, $\omega = 175$, and $\omega = 48$, respectively. The full diamonds represent the experimental data points at $\omega = 241$. Set (b) is for the boehmite cakes at pH = 7.0. The solid line and the open diamonds represent the calculated curves for $\omega = 241$ and $\omega = 175$, respectively. The full circles represent the experimental data points at $\omega = 241$. Set (c) is for the boehmite cakes at pH = 5.5. The solid line and the open circles represent calculated curves for $\omega = 241$ and $\omega = 175$. The full squares represent the experimental points at $\omega = 241$. All the curves for alumina cakes collapse onto one single curve. So do all the curves for boehmite cakes at pH = 7.0 and all the curves for boehmite cakes at pH = 5.5. Fig. 1 clearly shows that for cakes that have the same exponent n , the relative density change $\phi(z)/\phi_{\max}$ has a universal dependence on z/z_m . Meanwhile, the positions of the visual cake tops are indicated as α for the alumina cake at $\omega = 241$, as β for the boehmite cake at pH = 7.0 and as γ for the boehmite cake at $\omega = 241$. z_m may not coincide with the position of the visual cake top. For a large n (i.e., alumina cakes), z_m is close to the position of the visual cake top. As n is decreased, the gap between z_m and the position of the visual cake top is widened. This trend is in agreement with the experimental observations: For alumina at pH = 7.0, the supernatant is clear and the interface is sharp between the cake and the supernatant whereas for boehmite cakes, especially, at pH = 5.5, the supernatant becomes very cloudy and the cake-supernatant interface very diffuse.

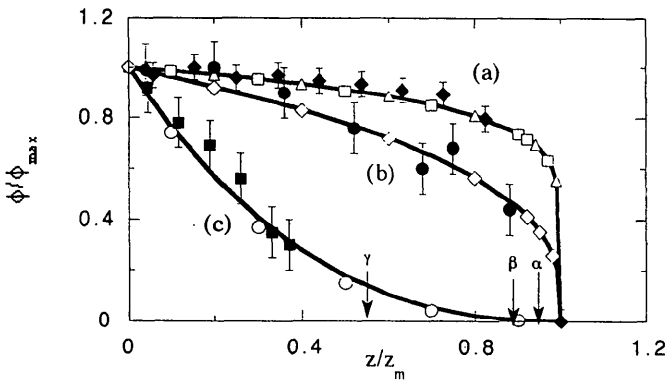


Figure 1: $\phi(z)/\phi_{\max}$ vs. z/z_m . Set (a) is for alumina at pH = 7.0. The solid line, the open triangles, and the open squares are calculated values for $\omega = 241$, 175, and 48 respectively. Set (b) is for boehmite at pH = 7.0. The solid line, the open diamonds are the calculated values for $\omega = 241$ and 175, respectively. Set (c) is for boehmite at pH = 5.5. The solid line and the open circles are for the calculated values at $\omega = 241$ and 175, respectively. The data points with error bars are from experiments at $\omega = 241$. The arrows indicate the experimental visual cake tops at $\omega = 241$: α for (a), β for (b), and γ for (c).

To compare the universal $\phi(z)/\phi_{\max}$ vs. z/z_m curves shown in Fig. 1 with Eq. (7), we replot the three solid curves of Fig. 1 in Fig. 2: (a) for alumina cakes, (b) for boehmite cakes at pH = 7.0, and (c) for boehmite cakes at pH = 5.5. Also plotted are open circles representing $[1 - (z/z_m)]^{1/(n-1)}$ at selected values of z/z_m . The three curves are indeed well described by $[1 - (z/z_m)]^{1/(n-1)}$ and the relative density drop within the main portion of the cake, e.g., $0 < z < 0.8 z_m$, increases as the value of n decreases. Note that $n = 2$ is a boundary for the shapes of the density profiles. For $n > 2$, such as in the alumina cakes at pH = 7.0 and boehmite cakes at pH =

7.0, $1/(n-1)$ is smaller than unity and thus the $\phi(z)/\phi_{\max}$ -vs- z/z_m curve is a convex one. For $n < 2$, such as in the boehmite cakes at pH = 5.5, $1/(n-1)$ is greater than unity and therefore, the -vs- z/z_m curve is a concave one. The result of a concave $\phi(z)/\phi_{\max}$ -vs- z/z_m curve is that the cake-supernatant boundary tends to be diffuse and the supernatant cloudy as observed in the boehmite system at pH = 5.5.

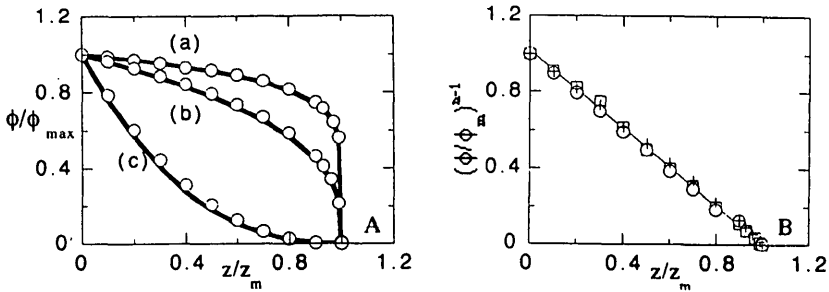


Figure 2: (A) Comparison of $\phi(z)/\phi_{\max}$ with $(1-z/z_m)^{1/(n-1)}$. The solid lines are replotted from Fig. 1. The open circles represent $(1-z/z_m)^{1/(n-1)}$ at selected values of z/z_m . (B) $(\phi(z)/\phi_{\max})^{n-1}$ vs. z/z_m as replotted from (A) for selected values of z/z_m : open squares for solid line (a), crosses for solid line (b), and open circles for solid line (c).

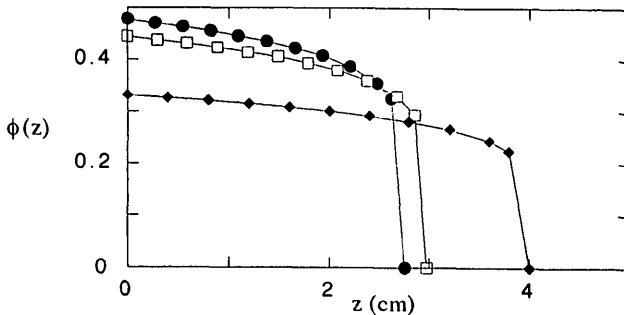


Figure 3: $\phi(z)$ vs. z of alumina cakes at various ω . The full circles denote $\omega = 241$, the open squares $\omega = 175$, and the full diamonds $\omega = 48$.

Even though we showed that $\phi(z)/\phi_{\max}$ can be described as a universal function $[1 - (z/z_m)]^{1/(n-1)}$, we note that the values of ϕ_{\max} and z_m vary with the suspension conditions and the centrifugation frequency. For example, at $\omega = 241$, $\phi_{\max} = 48$ vol%, 6.4 vol% and 7.8 vol% for the alumina cake, the boehmite cake at pH = 7.0, and the boehmite cake at pH = 5.5. Meanwhile, for the same suspension conditions, ϕ_{\max} increases with an increasing ω as shown in Fig. 3 where $\phi(z)$ vs. z of alumina cakes at various ω are plotted. Note that as a consequence of the universal dependence of $\phi(z)/\phi_{\max}$ on z/z_m , the density gradient actually increases despite that

the average cake density increases with an increasing ω (as depicted in Fig. 3). The reason is that a higher centrifugation frequency gives not only a higher ϕ_{\max} but also a smaller z_m . As a result, the density gradient increases with an increasing ω .

CONCLUDING REMARKS

We have examined the equilibrium-state density profiles of flocculated centrifuged cakes both theoretically and experimentally. Theoretically, the density profiles were obtained by implementing the experimentally obtained power-law pressure-density relationships $P_{s,m} = \beta \phi_{\text{ave}}^n$ into the general differential equations for centrifugation with appropriate boundary conditions. We show that the density profiles $\phi(z)$ vs. z can be described in a simple form as $\phi(z)/\phi_{\max} = [1 - (z/z_m)]^{1/(n-1)}$. The calculated density profiles were shown to be in good agreement with the experimental ones. Consequently, the relative pressure can be expressed as $P(z)/P_{\max} = [1 - (z/z_m)]^{n/(n-1)}$.

The form $\phi(z)/\phi_{\max} = [1 - (z/z_m)]^{1/(n-1)}$ can also describe the density profiles of sedimented cakes provided the pressure-density relationship of a sedimented cake is also a power-law function $P = \beta \phi^n$.⁸ While the $[1 - (z/z_m)]^{1/(n-1)}$ dependence of the relative density $\phi(z)/\phi_{\max}$ is an approximation for centrifuged cakes, it is exact for sedimented cakes.⁸ Furthermore, the uniform density profiles observed in the sedimented cakes of dispersed suspensions^{1,2} can also be described by this $\phi(z)/\phi_{\max} = [1 - (z/z_m)]^{1/(n-1)}$ form with n approaching ∞ , which is consistent with the observation that the cake density of dispersed suspensions is independent of the applied pressure.^{3,5}

ACKNOWLEDGEMENT

This work was supported by the Air Force Office of Scientific Research (AFOSR) under Grant No. AFOSR-91-0040.

REFERENCES

1. C. H. Schilling, G. L. Graff, W. D. Samuels, and I. A. Aksay, pp. 239-51 in *Atomic and Molecular Processing of Electronic and Ceramic Materials: Preparation, Characterization, and Properties* (Materials Research Society, Pittsburgh, PA, 1988), *MRS Conf. Proc.*, edited by I. A. Aksay, G. L. McVay, T. G. Stoebe, and J. F. Wager.
2. F. M. Auzerais, R. Jackson, W. B. Russel, and W. F. Murphy, "The transient settling of stable and flocculated dispersions," *J. Fluid Mech.* **221**, 613-39 (1990).
3. W.-H. Shih, S. I. Kim, W. Y. Shih, C. H. Schilling, and I. A. Aksay, *MRS Symp. Proc.*, **180**, 167 (1990).
4. W.-H. Shih, J. Liu, W. Y. Shih, S. I. Kim, M. Sarikaya, and I. A. Aksay, *MRS Symp. Proc.*, **155**, 83 (1989).
5. W.-H. Shih, W. Y. Shih, S. I. Kim, J. Liu, and I. A. Aksay, *Phys. Rev. A*, **42**, 4772 (1990).
6. W. Y. Shih, W.-H. Shih, and I. A. Aksay, *MRS Symp. Proc.*, **195**, 477 (1990).
7. F. M. Tiller, C. S. Yeh, C. D. Tsai, and W. Chen, *Filtration & Separation*, **24**, 121 (1987).
8. W.-H. Shih, W. Y. Shih, S. I. Kim, and I. A. Aksay, to be published.